Metallophysics and Advanced Technologies
Металофіз. новітні технол.
Metallofiz. Noveishie Tekhnol.
2021, vol. 43, No. 3, pp. 355–365
https://doi.org/10.15407/mfint.43.03.0355
Reprints available directly from the publisher

PACS numbers: 06.60.Vz, 62.20.M-, 68.08.De, 81.05.Ni, 81.40.Ef, 81.40.Np

Formation of Structure and Properties of Boron-Rich Fe–B–C Alloys Alloyed with Cr, V, Nb or/and Mo

O. V. Sukhova

Oles Honchar Dnipro National University,
72 Gagarin Ave.,
UA-49010 Dnipro, Ukraine

The effects of substitution of Fe in the boron-rich Fe–B–C alloys, containing 10.0–14.0% B and 0.1–1.2% C, 0–5.0 % Cr, V, Mo or/and Nb (in % wt.), are studied with combined analysis of optical microscopy, X-ray diffractometry, scanning electron microscopy, energy dispersive spectroscopy. The microstructure of the master Fe–B–C alloys consists mainly of primary dendrites of Fe(B, C) solid solution and Fe_2(B, C) crystals peritectically formed from Fe(B, C) phase and the rest of the melt. As found, chromium or vanadium have high solubility in the constituent phases of the Fe–B–C alloys, with preferential solubility observed in the Fe(B, C) dendrites, where Cr or V occupy Fe positions. The addition of Cr or V to the Fe–B–C alloys helps to modify their brittleness: while it slightly decreases microhardness values, addition of these elements notably improves the fracture toughness of the constituent phases. Molybdenum or niobium are shown to be present in secondary phases identified as Mo_2B, Mo_2(B, C) or NbB_2, respectively. The level of Mo or Nb contents in the Fe(B, C) and Fe_2(B, C) solid solutions and quantity of the observed secondary phases indicate a very small Mo and no Nb solubility in the constituent phases. The Mo or Nb enhances a hardness of the master Fe–B–C alloy due to secondary phases' precipitation. To enhance performance characteristics of the boron-rich Fe–B–C alloys, the 1.0–2.0% Cr, 0.5–1.0% V, 1.0–3.0% Nb, 1.0–3.0% Mo are simultaneously added to the master alloy. The properties improve due to the formation of Cr- and V-containing Fe_2(B, C) and Fe(B, C) solid solutions as well as Mo- and Nb-based secondary phases. The developed multicomponent alloy is recommended as a filler of macroheterogeneous composite coatings for strengthening of parts

Corresponding author: Olena Viktorivna Sukhova
E-mail: sukhovaya@ukr.net

Citation: O. V. Sukhova, Formation of Structure and Properties of Boron-Rich Fe–B–C Alloys Alloyed with Cr, V, Nb or/and Mo, *Metallofiz. Noveishie Tekhnol.*, **43**, No. 3: 355–365 (2021), DOI: 10.15407/mfint.43.03.0355.

working in abrasive or gas-abrasive media at elevated temperatures.

Key words: boron-rich iron-based alloys, alloying elements, microstructure, solid solutions, secondary phases, mechanical properties.

Вивчено вплив заміщення Fe у високобористих стопах Fe–B–C, що містять 10,0–14,0% B та 0,1–1,2% C, 0–5,0% Cr, V, Mo або/та Nb (у % ваг.), із застосуванням методів оптичної мікроскопії, рентґеноструктурного аналізу, сканувальної електронної мікроскопії, рентґеноспектрального мікроаналізу. Мікроструктура базових стопів Fe–B–C складається з первинних дендритів твердого розчину Fe(B, C) та кристалів Fe_2(B, C), що утворюються за перитектичною реакцією між фазою Fe(B, C) та рідиною. Встановлено, що хром та ванадій мають високу розчинність у структурних складових стопів Fe–B–C, причому Cr та V в більшій кількості розчиняються в дендритах Fe(B, C), займаючи позиції атомів Fe. Додавання Cr або V до стопів Fe–B–C дозволяє зменшити їх крихкість: незначно знижуючи мікротвердість структурних складових, ці елементи значно підвищують їх коефіцієнт тріщиностійкості. Показано, що молібден та ніобій переважно входять до складу вторинних надлишкових фаз, ідентифікованих у структурі як Mo_2B, Mo_2(B, C) або NbB_2 відповідно. Вміст Mo та Nb в твердих розчинах Fe(B, C) та Fe_2(B, C), а також кількість утворюваних ними вторинних фаз свідчать про низьку розчинність Mo та відсутність розчинності Nb в цих структурних складових. Mo та Nb збільшують твердість базового стопу Fe–B–C завдяки виділенню вторинних фаз. З метою підвищення експлуатаційних властивостей базових високобористих стопів Fe–B–C до їх складу одночасно додавали 1,0–2,0% Cr, 0,5–1,0% V, 1,0–3,0% Nb, 1,0–3,0% Mo. Покращення властивостей забезпечується формуванням Cr- та V-вмістних твердих розчинів Fe_2(B, C) та Fe(B, C), а також вторинних фаз на основі Mo та Nb. Розроблений багатокомпонентний стоп рекомендований в якості наповнювача макрогетерогенних композиційних покриттів, призначених для зміцнення поверхонь деталей, що працюють в абразивних або газоабразивних середовищах за підвищених температур.

Ключові слова: високобористі залізні стопи, леґуючі елементи, мікроструктура, тверді розчини, вторинні фази, механічні властивості.

(Received May 5, 2020; in final version, February 11, 2021)

1. INTRODUCTION

Boron-rich Fe–B–C alloys for industrial applications may be efficiently utilized since the alloys have thermal stability to resist abrasive and gas-abrasive wear, oxidation and corrosion at elevated temperatures [1–5]. However, under impact loads these alloys become inadequate due to their low resistance to cracking. It results in the loss of the valuable properties and severely limits the high temperature characteristics of the alloys restricting their use in critical applications. However, the combination of excellent performance properties makes them the

perspective materials for surface application [6–13].

Recent results have indicated that the alloying of the Fe–B–C alloys not only affects their structure, but also significantly decreases their brittleness [14–19]. To obtain high-quality coatings based on Fe–B–C alloys with good performance properties, it is important to be aware of their microstructure. Since only a few studies have been carried out and are in some aspects contradictory, especially in the alloyed Fe–B–C system, experiments were conducted to determine the alloying effects on the structure and the properties of boron-rich Fe–B–C alloys.

2. EXPERIMENTAL DETAILS

The composition of Fe–B–C alloys, determined by chemical and spectral analyses, was within the concentration range of 10.0–14.0% B, 0.1–1.2 % C, 0–5.0 % Me (where Me—Cr, V, Mo, or/and Nb), Fe—the remainder (in % wt.). The specimens were prepared by melting the constituent elements of high purity (99.99 %) in a Tamman furnace and solidified at cooling rate of 10 K/s.

For microstructural characterization, metallographic sections were observed by light metallographic microscope Neophot-32 and scanning electron microscope Jeol-2010 F (SEM) equipped with energy-dispersive spectrometer (EDS). Composition and lattice parameters of the phases in the investigated alloys as a function of composition were determined by X-ray diffractometer HZG-4A with CuK_α radiation. The melting temperature of the alloys was measured by differential thermal analysis at 5 K/min heating (cooling) rate. To evaluate oxidation resistance factor, polished samples were oxidized in air at 1273 K for 2 hours.

Compression tests were performed at room temperature on samples ($10\times10\times20$ mm^3) deformed along the longitudinal axis. The load was applied up to fracture of the specimens. The Vickers microhardness (H_μ) was measured using device PMT-3 from at least 10 different indentations, and the fracture toughness (K_{1C}) was evaluated from the crack length initiated at the corners of the Vickers microindentation using an empirical equation proposed in [20]:

$$K_{1C} = \frac{0.15k(2c/d)^{-3/2}}{F} H_\mu \sqrt{d/2},\ F = 3,\ k = 3.2,$$

where d is the indentation diagonal, c is the crack length.

3. RESULTS AND DISCUSSION

The conducted investigations show that Fe_2(B, C) and Fe(B, C) solid solutions are the major constituents of the master boron-rich Fe–B–C

alloys within the concentration range of 10.0–14.0% B, 0.1–1.2% C, Fe—the remainder (in % wt.). The primary solid solution Fe(B, C) arises on the base of iron monoboride and grows in the form of three-dimensional dendrite [21, 22]. Solid solution Fe_2(B, C) is formed afterwards via peritectic reaction L + Fe(B, C) → Fe_2(B, C). The following changes have been observed after alloying the Fe–B–C alloys with 0–5.0% of one of the following elements: V, Cr, Mo or Nb.

Figure 1 shows micrographs and the corresponding X-ray element-distribution maps of the alloys. A well-defined dendritic structure can

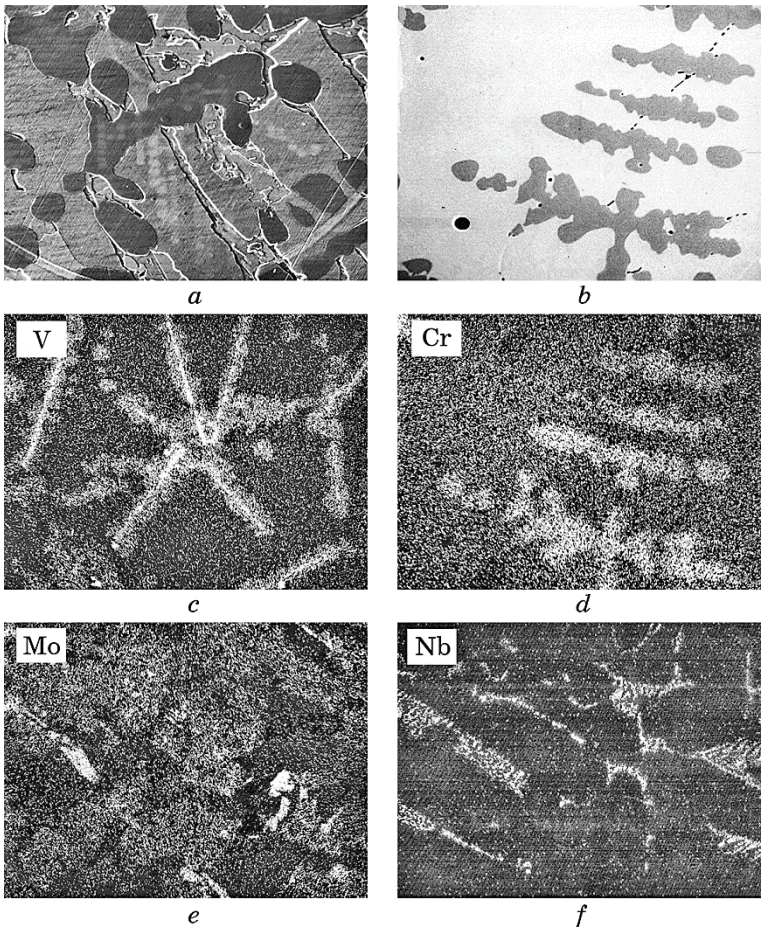

Fig. 1. SEM micrographs (*a*, *b*) and elemental EDS X-ray mappings (*c*–*f*) of polished cross-sections of Fe–12.1B–0.1C sample alloyed with 5% of V, Cr, Mo or Nb: *a*—back-scattered image; *b*—second electron image; *c*—distribution of Cr; *d*—distribution of V; *e*—distribution of Mo; *f*—distribution of Nb.

TABLE 1. The lattice parameters, dendrite parameters and mechanical properties of Fe(B, C) dendrites in the Fe–12.1B–0.1C sample alloyed with 5% of V, Cr, Mo or Nb.

Alloying element	Rhombic lattice parameters, nm			Dendrite parameters, μm		H_μ, GPa	K_{1C}, MPa·m$^{1/2}$
	a	b	c	d_0	l_0		
without	0.55051 ± ± 0.00061	0.40628 ± ± 0.00097	0.29480 ± ± 0.00007	29.9 ± ± 0.6	4.9 ± ± 0.2	17.1 ± 0.3	2.3 ± 0.1
V	0.55061 ± ± 0.00028	0.40480 ± ± 0.00034	0.29652 ± ± 0.00010	29.8 ± ± 0.5	4.4 ± ± 0.1	16.8 ± 0.5	3.6 ± 0.2
Cr	0.55111 ± ± 0.00024	0.40626 ± ± 0.00016	0.29645 ± ± 0.00007	29.4 ± ± 0.6	4.6 ± ± 0.1	16.5 ± 0.3	3.8 ± 0.2
Mo	0.55051 ± ± 0.00034	0.40650 ± ± 0.00062	0.29472 ± ± 0.00020	23.6 ± ± 0.5	3.1 ± ± 0.1	17.3 ± 0.2	2.1 ± 0.1
Nb	0.55034 ± ± 0.00021	0.40622 ± ± 0.00071	0.29498 ± ± 0.00032	22.4 ± ± 0.4	2.4 ± ± 0.5	17.1 ± 0.4	2.2 ± 0.1

be found on all the polished cross-sections. These dendrites consist entirely of iron monoboride crystals, which is consistent with the result obtained by the XRD technique.

Element-distribution map analysis has revealed that vanadium, dissolved to the amount of 2.0–5.0% wt., gives rise to a non-homogeneous structure of the Fe(B, C) solid solution (Fig. 1, *c*). A light needle-like phase is clearly seen in the dendrite interior due to preferential solubility of vanadium in this phase. The EDS estimation of its composition gives Fe(B, C)$_2$. It appears that vanadium substitution for iron causes a shift in the alloy composition. It can be assumed that the first solid phase forming from the liquid is Fe(B, C)$_2$, and Fe(B, C) phase is the product of a peritectic reaction of the type: L + Fe(B, C)$_2$ → → Fe(B, C). Therefore, part of the liquid solidifies to produce a cored structure consisting of the Fe(B, C)$_2$ phase surrounded by the Fe(B, C) shell because there is not enough time for peritectic reaction to go to completion, and not all the liquid is consumed by reacting with Fe(B, C)$_2$ to produce Fe(B, C) crystals. Afterwards Fe$_2$(B, C) crystals are formed as the result of the peritectic reaction between the Fe(B, C) and liquid. The lowest solubility of vanadium is observed in the Fe$_2$(B, C) phase which is consistent with the results of the determination of the lattice parameters of Fe$_2$(B, C) and Fe(B, C) crystals measured by XRD method (Tables 1, 2).

Chromium completely dissolves in the Fe–B–C alloys, as illustrated in Fig. 1, *d*. This element, that has some solubility in Fe$_2$(B, C) phase, is mainly accommodated in the structure of Fe(B, C) crystals. Chromium as well as vanadium occupy iron positions in the crystalline lattices of

TABLE 2. The lattice parameters and mechanical properties of $Fe_2(B, C)$ crystals in the Fe–12.1B–0.1C sample alloyed with 5% of V, Cr, Mo or Nb.

Alloying element	Tetragonal lattice parameters, nm			H_μ, GPa	K_{1C}, MPa·m$^{1/2}$
	a	c	c/a		
without	0.51130 ± 0.00008	0.42399 ± 0.00035	0.8292	15.8 ± 0.3	2.2 ± 0.1
V	0.51161 ± 0.00006	0.42449 ± 0.00013	0.8297	15.4 ± 0.2	3.0 ± 0.2
Cr	0.51176 ± 0.00011	0.42463 ± 0.00040	0.8297	15.0 ± 0.1	2.8 ± 0.2
Mo	0.51184 ± 0.00004	0.42435 ± 0.00047	0.8291	15.7 ± 0.2	2.2 ± 0.1
Nb	0.51133 ± 0.00008	0.42404 ± 0.00029	0.8293	15.8 ± 0.1	2.1 ± 0.1

the constituent phases forming substitutional solid solutions as the results of XRD measurements show (Tables 1, 2). Besides, alloying with chromium and vanadium does not noticeably influence a diameter of the secondary arms (d_0) and interdendritic distance (l_0) for Fe(B, C) dendrites (Table 1). Vanadium and chromium slightly decrease microhardness H_μ but significantly enhance the fracture toughness K_{1C} of the constituent phases (Tables 1, 2).

The structure of Fe–B–C samples alloyed with molybdenum yields some significant changes. Molybdenum slightly dissolves in Fe(B, C) crystals, and only negligible content of this element is revealed in $Fe_2(B, C)$ solid solution by EDS analysis (Fig. 1, *e*). This implies that Mo is continually being transported in the melt ahead of the moving solid-liquid interface after the primary phases have formed. A portion of Mo becomes incorporated into the solidified phases, but solubility limit forces the remaining solute into the residual liquid. As a result, the secondary crystals of Mo_2B and $Mo_2(B, C)$ are seen at the $Fe_2(B, C)$ boundaries.

The boron-rich Fe–B–C alloys have no noticeable solubility for niobium. This element has been shown to be present in secondary NbB_2 phase. No significant shift of lattice parameters of the $Fe_2(B, C)$ and Fe(B, C) solid solutions can be spotted on the X-ray diffraction patterns with increasing percent of niobium (Tables 1, 2). Niobium as well as molybdenum cause substantial decrease in the dendrite parameters of Fe(B, C) crystals, as shown in Table 1. These elements slightly influence the microhardness and the fracture toughness of the major phases (Tables 1, 2), but they may affect mechanical properties via precipitation of secondary phases.

Based on obtained results, 1.0–2.0% Cr, 0.5–1.0% V, 1.0–3.0% Nb, and 1.0–3.0% Mo have been simultaneously added to the master Fe–B–C alloy in order to enhance its performance characteristics. The multicomponent alloy exhibits complex heterogeneous structure (Fig. 2). EDS measurements show that vanadium and, in less quantity,

chromium are preferentially dissolved in Fe(B, C) dendrites (Fig. 3). These elements are also revealed in Fe_2(B, C) phase. Identical information is supplied by the element distribution charts (Fig. 2, *a*, *b*). Besides, the second phases are present throughout the samples: they exhibit a noticeably bright contrast than Fe_2(B, C) matrix (Fig. 2, *c*, *d*). The estimate compositions obtained are Mo_2B, Mo_2(B, C), and NbB_2. Niobium and molybdenum form secondary phases at the Fe_2(B, C) boundaries because very little or no these elements are left in the Fe(B, C) dendrites and Fe_2(B, C) matrix. The volume of these extra phases is less than 10%. So, the distribution of Cr is most homogeneous in the multicomponent alloy and the level of homogeneity increases in the order of Cr < V < Mo < Nb. Table 3 shows the performance properties of the alloy. Alloying elements significantly enhance the Rockwell hardness, compression strength and oxidation resistance. Furthermore, the melting temperature increases which is favourable for application of the multicomponent alloy as a filler of metal-matrix composites [23, 24].

The crystallization process of boron-rich Fe–B–C alloys simultaneously alloyed with Cr, V, Nb, and Mo may be assumed as follows. As Fe(B, C) and Fe_2(B, C) crystals grow from the liquid, they capture chromium and vanadium, with Cr- and V-containing solid solutions on

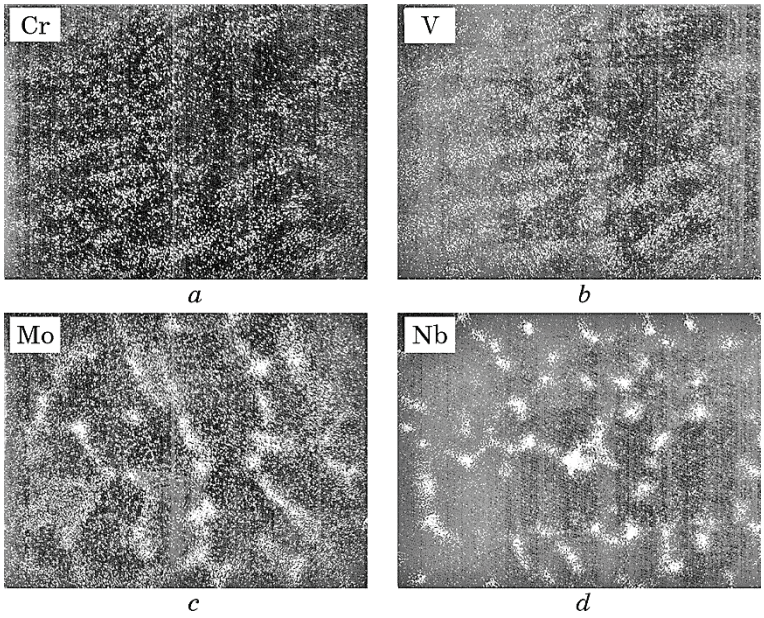

Fig. 2. Element-distribution maps of polished cross-section of the Fe–12.1B–1.1Cr–1.0V–1.2Nb–1.1Mo–0.1C alloy: *a*—distribution of Cr; *b*—distribution of V; *c*—distribution of Mo; *d*—distribution of Nb.

TABLE 3. The performance properties of Fe–10.3B–0.7C and Fe–10.3B–0.7C–Me alloys (where Me—1.5% Cr, 1.0% V, 3.0% Nb, 3.0% Mo).

Alloy	Hardness, *HRA*	Melting temperature, K	Oxidation resistance factor, relative units	Compression strength, MPa
Fe–B–C	82 ± 1	1723 ± 4	1.0	2010 ± 10
Fe–B–C–Me	85 ± 2	1748 ± 4	1.37 ± 0.15	2120 ± 10

their base being formed. Molybdenum and niobium are mainly dissolved in the liquid. As solidification progresses, the atoms of Mo and Nb are pushed out of the solid-liquid interface into the interdendritic regions of growing dendrites slowing their growth and causing noticeable refinement. Ultimately, with temperature further lowering, the remaining liquid, enriched by molybdenum and niobium, solidifies via eutectic reaction in which Mo_2B, $Mo_2(B, C)$ and NbB_2 secondary phases precipitate at the boundaries of $Fe_2(B, C)$ crystals.

In the first place, the propensity for the solutes to form solid solutions involves the crystallographic aspect. To estimate the solubility of the alloying elements, the $(r_0 - r)/r_0$ ratio should be of use, where r—atomic radius of the solvent, r_0—atomic radius of the solutes. Compar-

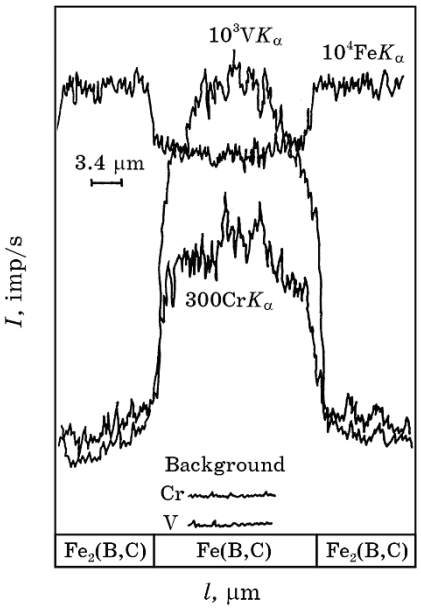

Fig. 3. Elemental profiles for Cr and V in the Fe–12.1B–1.1Cr–1.0V–1.2Nb–1.1Mo–0.1C alloy.

ison of this radius ratio for studied alloying elements exhibits the following sequence Cr → V → Mo → Nb. Correspondingly, their solubility in the structural constituents of the Fe–B–C alloys decreases.

The Cr and V solute atoms incorporate into the solvent Fe(B, C) and Fe_2(B, C) crystalline lattices substitutionally by replacing iron atoms in the crystalline lattices. It is also obvious that chromium and vanadium are preferentially dissolved in the rhombic lattice of iron monoboride than in more close-packed lattice of iron hemiboride. Compared with vanadium, chromium has smaller atomic radius and, therefore, affects the lattice parameters of the phases in a lower extent. Molybdenum and niobium do not noticeably dissolve in the lattices of Fe(B, C) and Fe_2(B, C) crystals forming secondary phases.

The alloying elements affect the microhardness and fracture toughness of the phases present in the Fe–B–C alloys by distorting their crystalline lattices. The local nonuniformity in the solvent lattices due to the solutes makes plastic deformation more difficult by impending dislocation motion. The change of the mechanical properties of FeB- and Fe_2B-based solid solutions may be explained considering the peculiarities of their electronic structure within the framework of configurational model of substance proposed by G. V. Samsonov [25]. Mechanical properties are determined primarily by the strength and directionality of the interatomic bonds. The stability of the iron borides depends on B–B and Fe–B bonds energy. The strength of these bonds is determined by the distraction of collectivized valence electrons of iron. The ions of V, Cr, Mo or Nb have p^6-shells and form to B the same interatomic bonds as Fe. As a result of the substitution of Fe by Cr or V the fewer bonding electrons take part in the electronic exchange. The B–B and Fe–B bonds become weaker and, therefore, the microhardness and the brittleness of the Cr- and V-containing solid solutions are found to decrease.

The probability that valence electrons of Mo and Nb are localized in the stable d^5-configurations is rather high. That is why, these elements act as electron acceptors. Any rearrangement of the bonding electrons in such system may result in the energetically non-advantageous destruction of the stable configurations. Therefore the solubility of Mo and Nb in Fe(B, C) or Fe_2(B, C) crystals is negligible or absent and they enhance the hardness with preserving the K_{1C} value by strengthening via the precipitation of secondary phases.

4. CONCLUSION

Substitution of Fe in boron-rich Fe–B–C alloys, containing 10.0–14.0% B, 0.1–1.2% C, Fe—the remainder, by 0–5.0% Cr, 0–5.0% V, 0–5.0% Nb or/and 0–5.0 % Mo (in % wt.) does not greatly affect the solidification morphology of the Fe(B, C) and Fe_2(B, C) solid solutions

that are major structural constituents of the alloys. The solidification process consists of the primary crystallization of Fe(B, C) dendrites and peritectic reaction forming the Fe_2(B, C) phase.

The study concerning the effect of chromium or vanadium shows that they have a high solubility in the Fe–B–C alloys. These elements are localized in the Fe(B, C) crystals in a high proportion and in the Fe_2(B, C) matrix in a lower content. Their atoms mainly substitute for the iron atoms in the crystalline lattices, which leads to weakening 'iron–boron' and 'boron–boron' bonds of the solid solutions. Therefore, alloying with chromium or vanadium enhances the fracture toughness of the constituent phases.

The negligible dissolution of molybdenum or niobium in the Fe–B–C alloys is responsible for the appearance of secondary phases, such as Mo_2B, Mo_2(B, C) or NbB_2, at the Fe_2(B, C) boundaries. It appears that Mo and Nb are affecting the solidification morphology while they are present as solutes in the liquid rather than as a heterogeneous nucleant. The result can be explained by electronic structure of these alloying elements that do not supply necessary electrons for the electronic exchange. Molybdenum or niobium influence the mechanical properties of the Fe–B–C alloys *via* precipitation of secondary phases that enhance hardness of the alloys.

When V, Cr, Nb, and Mo are simultaneously added to Fe–B–C alloy, the same primary and secondary phases are formed. As evidenced by the X-ray mappings, distribution of Cr is most homogeneous in the alloy and the level of homogeneity increases in the order of Cr < V < Mo < < Nb. The multicomponent alloy shows a relatively high melting temperature, hardness and fracture toughness, compression strength and oxidation resistance as compared with the master Fe–B–C alloy. These properties can be used for technological applications in the form of reinforcement particles in metal-matrix composite coatings where resistance to abrasive or gas-abrasive wear at elevated temperatures is required.

REFERENCES

1. X. Ren, H. Fu, J. Xing, Y. Yang, and S. Tang, *J. Mater. Res.*, **32**, No. 16: 3078 (2017).
2. A. Sudo, T. Nishi, N. Shirasu, M. Takano, and M. Kurata, *J. Nuclear Sci. Technol.*, **52**, No. 10: 1308 (2015).
3. P. Sang, H. Fu, Y. Qu, C. Wang, and Y. Lei, *Materialwissenschaft und Werkstofftechnik*, **46**, No. 9: 962 (2015).
4. Z. F. Huang, J. D. Xing, S. Q. Ma, Y. M. Gao, M. Zheng, and L. Q. Sun, *Key Eng. Mater.*, **732**: 59 (2017).
5. V. Homolova, L. Ciripova, and A. Vyrostkova, *J. Phase Equilibria Diff.*, **36**, No. 6: 599 (2015).
6. O. V. Sukhova, *Metallofiz. Noveishie Technol.*, **31**, No. 7: 1001 (2009)

(in Ukrainian).
7. O. V. Sukhova and Yu. V. Syrovatko, *Metallofiz. Noveishie Technol.*, **33**, Special Issue: 371 (2011) (in Russian).
8. I. M. Spiridonova, E. V. Sukhovaya, V. F. Butenko, A. P. Zhudra, A. I. Litvinenko, and A. I. Belyi, *Powder Metallurgy and Metal Ceramics*, **32**, No. 2: 45 (1993).
9. V. G. Efremenko, V. I. Zurnadzhi, Y. G. Chabak, O. V. Tsvetkova, and A. V. Dzherenova, *Mater. Sci.*, **53**: 67 (2017).
10. I. M. Spiridonova, E. V. Sukhovaya, S. B. Pilyaeva, and O. G. Bezrukavaya, *Metall. Min. Ind.*, No. 3: 58 (2002) (in Russian).
11. I. M. Spiridonova, O. V. Sukhova, and A. P. Vashchenko, *Metallofiz. Noveishie Technol.*, **21**, No. 2: 122 (1999) (in Russian).
12. Z. A. Duriagina, T. M. Kovbasyuk, and S. A. Bespalov, *Uspekhi Fiziki Metallov*, **17**, No. 1, 29 (2016).
13. Z. A. Duryagina, S. A. Bespalov, V. Ya. Pidkova, and D. Yu. Polockyj, *Metallofiz. Noveishie Technol.*, **33**, Special Issue, 393 (2011) (in Ukrainian).
14. A. A. Sorour, A. S. Adeniyi, M. A. Hussein, C. P. Kim, and N. M. Al-Aqeeli, *Proc. of Conf. 'Materials Science and Technology' (Oct. 14–18, 2018)* (Columbus, Ohio, USA: 2018), p. 1454.
15. W. Shenglin, *China Welding*, **27**, No. 4: 46 (2018).
16. P. Christodoulou and N. Calos, *Mater. Sci. Eng. A*, **301**, No. 2: 103 (2001).
17. M. Zhang, X. Wang, S. Liu, and K. Qu, *J. Rare Earths*, **5**: 13 (2019).
18. S. Egashira, T. Sekiya, T. Ueno, and M. Fujii, *Mech. Eng. J.*, **6**, No. 6, 19-00297 (2019).
19. Z. Chen, S. Miao, L. Kong, X. Wei, F. Zhang, and H. Yu, *Materials*, **13**, No. 4: 975 (2020).
20. N. V. Novikov, S. N. Dub, and S. I. Bulychov, *Ind. Lab. Diagn. Mater.*, No. 7: 60 (1988) (in Russian).
21. I. M. Spiridonova, E. V. Sukhovaya, and V. P. Balakin, *Metallurgia*, **35**, No. 2: 65 (1996).
22. O. V. Sukhova, *Phys. Chem. Solid St.*, **21**, No. 2: 355 (2020).
23. E. V. Sukhovaya, *J. Superhard Mater.*, **35**, No. 5: 277 (2013).
24. O. V. Sukhova, V. A. Polonskyy, and K. V. Ustinova, *Voprosy Khimii i Khimicheskoy Tekhnologii*, **121**, No. 6: 77 (2018).
25. G. V. Samsonov, *Konfiguratsionnaya Model Veshchestva* [Configurational Model of Substance] (Kyiv: Naukova Dumka: 1971) (in Russian).